

한국표면공학회지
Journal of the Korean Institute of Surface Engineering
Vol. 34, No. 5, Oct. 2001
<연구논문>

The Oxidation of Functionally Gradient NiCrAlY/YSZ Coatings

K. B. Park*, H. S. Choi**, H. J. Kim***, D. B. Lee*

* Center for Advanced Plasma Surface Technology, Sungkyunkwan University,
Suwon 440-746, Korea

** Division of Materials Science and Engineering, Hanyang University,
Seoul 133-791, Korea

*** Center for Advanced Plasma Surface Technology, RIST, Pohang 790-330, Korea

Abstract

Functionally gradient NiCrAlY/ZrO₂-Y₂O₃ and NiCrAlY/ZrO₂-CeO₂-Y₂O₃ coatings were prepared by APS. The as-sprayed microstructure consisted of metal-rich and ceramic-rich regions, between which Al₂O₃-rich layers existed owing to the oxidation during APS. During oxidation between 900 and 1100°C in air, the pre-existing Al₂O₃-rich scales grew, due mainly to the preferential reaction of Al with inwardly transporting oxygen along the heterogeneous phase boundaries. As the amount of ceramics in the coating increased, the oxidation resistance increased.

1. INTRODUCTION

The coatings used for high-temperature components in gas turbines and diesel engines are generally composed of refractory ceramic top-coat such as yttria-stabilized zirconia (YSZ) and metallic bond-coat such as NiCrAlY¹⁾. The top-coat serves as both thermal and chemical barriers, while the bond-coat enables the top-coat to bond to the base alloy. But, the oxidation of bond-coat and the subsequent spallation of the top-coat are problems during service^{2, 3)}. Hence, functionally gradient coatings that gradually change their composition were designed to provide a good bonding strength between the top-coat and the bond-coat. This study aims at illustrating the oxi-

dation behavior of functionally gradient NiCrAlY/YSZ composite coatings.

2. Experimental procedures

To simulate functionally gradient coatings, coating compositions that are listed in Table 1

Table 1. Chemical composition of the prepared coatings. X = (ZrO₂-8Y₂O₃); Y = (ZrO₂-25CeO₂-2.5Y₂O₃); Z = (Ni-22Cr-10Al-1Y).

Designation	Composition (wt%)
coating 1	5% X + 75% Z
coating 2	50% X + 50% Z
coating 3	75% X + 25% Z
coating 4	25% Y + 75% Z
coating 5	50% Y + 50% Z
coating 6	75% Y + 25% Z

Table 2. Spaying parameters for the prepared coatings

Coating materials	Ampere (A)	Gas flow rate (SCFH)			Feed rate (g/min)	Spray distance (mm)
		Primary gas (Ar)	Secondary gas (N ₂)	Carrier gas (Ar)		
ZrO ₂ -Y ₂ O ₃ /NiCrAlY	500	75	20	12	40	100
ZrO ₂ -CeO ₂ -Y ₂ O ₃ /NiCrAlY	500	75	20	12	40	100

were prepared by APS. The spaying condition is shown in Table 2. The atomized, spherical starting powders were ZrO₂-8Y₂O₃ (11-125 μm), ZrO₂-25CeO₂-2.5Y₂O₃ (16-90 μm) and Ni-22Cr-10Al-1Y (56-106 μm). These ceramic and metallic powders were deposited simultaneously using 2 individual feeding systems to predetermined compositions to nominal thickness of 500 μm onto SS41 substrates. The deposited specimens were cut into a plate-like shape approximately 7 mm × 15 mm, and the substrate was ground off. Then, both sides of the coatings were polished to a 2000 grit finish, degreased in acetone, and oxidized.

The isothermal and cyclical oxidation tests were performed at 900, 1000, and 1100°C in static air using a muffle furnace. For cyclic oxidation tests, the specimens were oxidized for 1 h, cooled quickly to room temperature, weighed and returned to the furnace, for a total exposure of 100 h (100 cycles). The weight gains by oxidation were measured using a microbalance as a function of time. The specimens were investigated by SEM/EDS, and XRD.

3. Results and discussion

Fig. 1(a) shows a typical morphology of the APS'ed coating. The white areas are ceramic-rich regions, the gray areas are metal-rich regions, and the dark areas are Al₂O₃-rich regions, which was evidenced from EDS analyses. Some crack-

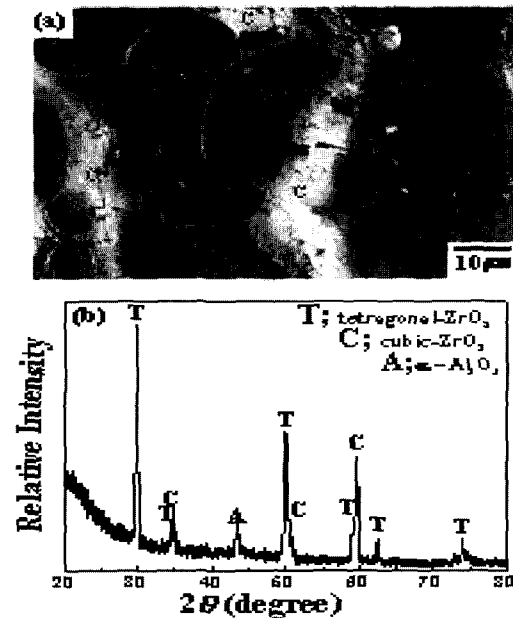


Fig. 1 As-APS'ed 'coating 3': (a) SEM cross-sectional image; and (b) X-ray diffraction pattern. M = metal-rich region, C = ceramic-rich region, A = Al₂O₃-rich region.

like inter-splats and round voids are formed owing to the APS followed by rapid cooling. Aluminum in NiCrAlY was oxidized selectively. From Fig. 1(b), it is seen that the coating is composed of tetragonal-ZrO₂, cubic-ZrO₂, and α-Al₂O₃. No Y₂O₃ and CeO₂ were detected probably due to their dissolution in ZrO₂. Clearly, the Al₂O₃-rich regions consisted mainly of α-Al₂O₃.

Fig. 2 shows the long-time isothermal oxidation kinetics of the coatings in the temperature range of 900-1100°C in air. Each data point was obtained from each coating that was oxidized for

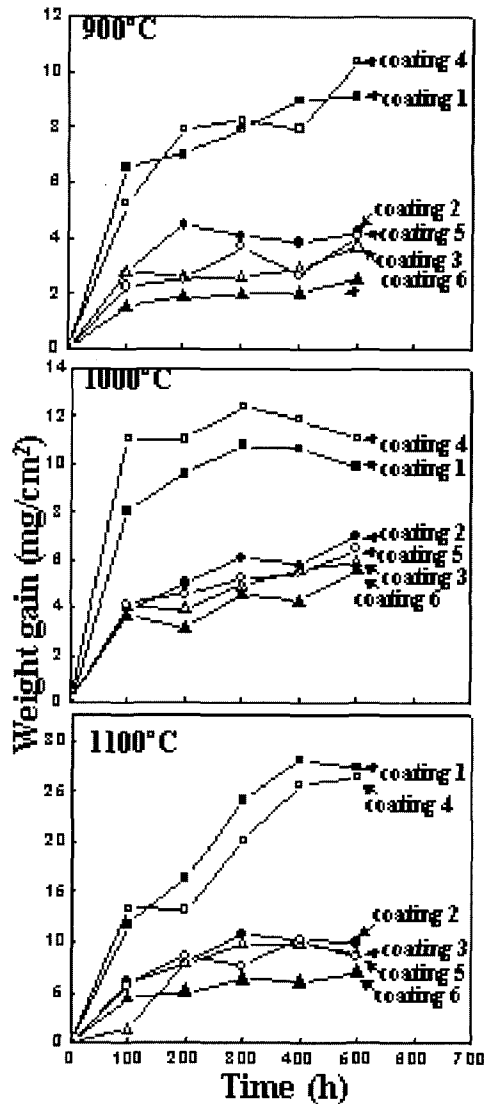


Fig. 2 Weight change vs. time curves of prepared coatings during isothermal oxidation at 900, 1000 and 1100°C in air.

a predetermined time at each temperature. It is noted that the composition of each coating was not ideally uniform and the amount of voids and microcracks was different for each coating. There also can be an error in measuring the surface area of each sample. All these facts can give some errors in measuring the actual weight gain per

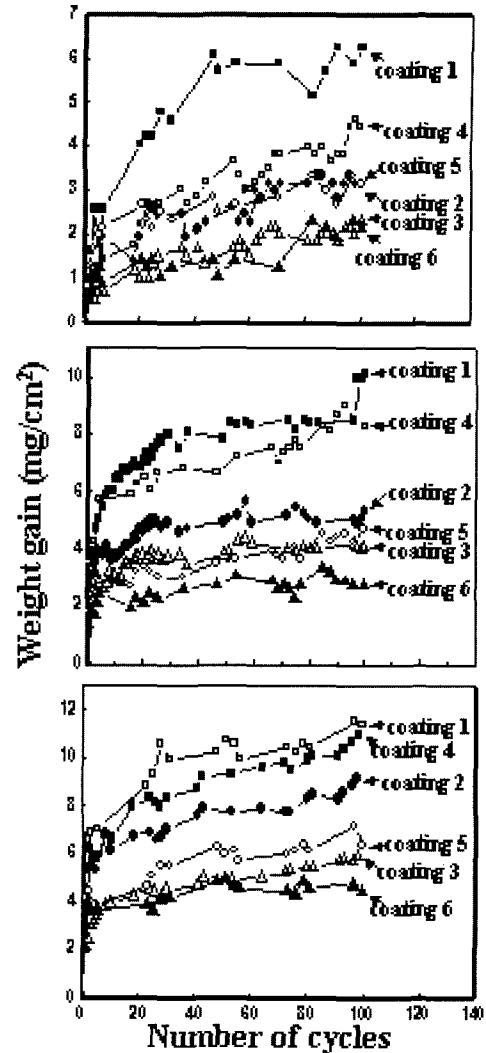


Fig. 3 Weight change vs. time curves of prepared coatings during cyclic oxidation at 900, 1000 and 1100°C in air.

unit area for each coating. Nevertheless, it is seen that the weight gains increased as the oxidation temperature and time increased. Generally, less oxidation occurred as the amount of ceramic increased, owing to the decreased amount of oxidizing metallic elements in the coating. Particularly, the 'coating 6' displayed excellent oxidation resistance.

The cyclic oxidation test results are shown in Fig. 3. The general cyclic oxidizing tendency of prepared coatings was similar to that of isothermal oxidation. The oxidation resistance increased with increasing the ceramic content. The difference in the kind of employed ceramics, i.e., $(\text{ZrO}_2\text{-CeO}_2\text{-Y}_2\text{O}_3)$ and $(\text{ZrO}_2\text{-Y}_2\text{O}_3)$, did not appreciably affect the oxidation resistance of the coating. Repeated thermal cycles induced more thermal stress and made the coating more susceptible to breakage, causing more overall weight gains and weight fluctuations when compared to isothermal oxidation.

Fig. 4 show the SEM image and the corresponding EDS spectrum of the 'coating 6' after isothermal oxidation. The metal-rich regions (gray area) are completely surrounded by the ceramic-

rich regions (white area), because there are three times more ceramics than metals in the coating. Voids and microcracks are scattered over the whole area. In the EDS spectrum shown, carbon peak was obtained due to carbon sputtered on the SEM mount. As did in as-sprayed coatings, Al was preferentially oxidized along the phase boundaries of metal-rich and ceramic-rich regions. This principal oxidation mode prevailed over all the tested coatings, under any oxidizing conditions.

4. Conclusions

The as-sprayed NiCrAlY/PSZ consisted of metal-rich and ceramic-rich regions. Because of air spraying, an Al_2O_3 -rich layer was formed at the interface of those two regions. During oxidation, the Al_2O_3 -rich layer grew, and surrounded the metal-rich region. As the amount of ceramics in the coating increased, the oxidation resistance increased.

References

1. W. Beele, G. Marijnissen, A. van Lieshout, Surf. Coat. Technol. 120-121 (1999) 61
2. J. A. Haynes, E. D. Rigney, M. K. Ferber, W. D. Porter, Surf. Coat. Technol. 86-87 (1996) 102
3. D. Strauss, G. Muller, G. Schumacher, V. Engelko, W. Stamm, D. Clemens, W. J. Quaddakers, Surf. Coat. Technol. 135 (2001) 196

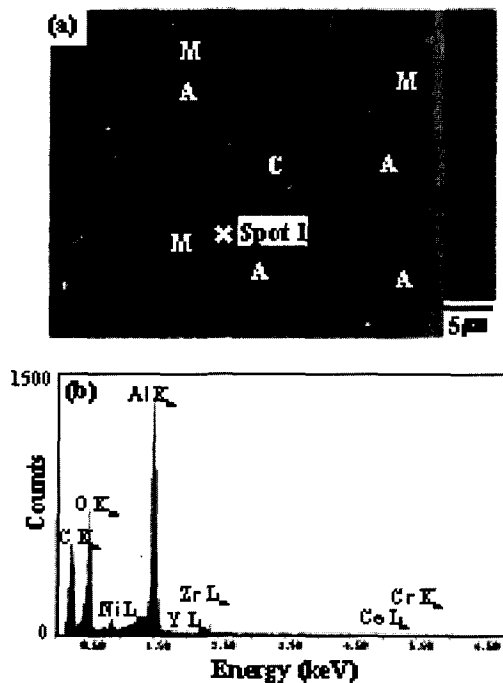


Fig. 4 (a) SEM image of 'coating 6' after isothermal oxidation at 1100°C for 500 h; and (b) EDS spectrum of spot 1.